RSC Advances

PAPER

View Article Online
View Journal | View Issue

Cite this: *RSC Adv.*, 2021, **11**, 26963

A nano-sized Cu-MOF with high peroxidase-like activity and its potential application in colorimetric detection of H_2O_2 and glucose†

Hao Yu,[a] Hanliu Wu,[a] Xuemei Tian,[a] Yafen Zhou,[a] Chunguang Ren*[b] and Zhonghua Wang *[a]

Peroxidase widely exists in nature and can be applied for the diagnosis and detection of H_2O_2, glucose, ascorbic acid and other aspects. However, the natural peroxidase has low stability and its catalytic efficiency is easily affected by external conditions. In this work, a copper-based metal–organic framework (Cu-MOF) was prepared by hydrothermal method, and characterized by means of XRD, SEM, FT-IR and EDS. The synthesized Cu-MOF material showed high peroxidase-like activity and could be utilized to catalyze the oxidation of *o*-phenylenediamine (OPDA) and 3,3′,5,5′-tetramethylbenzidine (TMB) in the presence of H_2O_2. The steady-state kinetics experiments of the oxidation of OPDA and TMB catalyzed by Cu-MOF were performed, and the kinetic parameters were obtained by linear least-squares fitting to Lineweaver–Burk plot. The results indicated that the affinity of Cu-MOF towards TMB and OPDA was close to that of the natural horseradish peroxidase (HRP). The as-prepared Cu-MOF can be applied for colorimetric detection of H_2O_2 and glucose with wide linear ranges of 5 to 300 μM and 50 to 500 μM for H_2O_2 and glucose, respectively. Furthermore, the specificity of detection of glucose was compared with other sugar species interference such as sucrose, lactose and maltose. In addition, the detection of ascorbic acid and sodium thiosulfate was also performed upon the inhibition of TMB oxidation. Based on the high catalytic activity, affinity and wide linear range, the as-prepared Cu-MOF may be used for artificial enzyme mimics in the fields of catalysis, biosensors, medicines and food industry.

Received 23rd June 2021
Accepted 30th July 2021

DOI: 10.1039/d1ra04877e

rsc.li/rsc-advances

1. Introduction

Metal–organic frameworks (MOFs) are crystalline porous framework materials that are formed with organic ligands and metal ions through coordination bonds with a periodic network structure.[1] MOFs have been widely used in catalysis,[2] sensing,[3] gas adsorption and separation,[4] luminescence[5] and other fields due to their large specific surface area, unsaturated sites, and structural and functional diversity.[6–8] MOFs materials have been shown to have great application prospects with more and more kinds of MOFs and their composite materials having been discovered. In the field of catalysis, MOFs with high catalytic efficiency have been reported. Qin *et al.* found that hollow mesoporous MOF exhibited superior catalytic performance when loading Pd nanoparticles toward benzyl alcohol oxidation.[9] Furthermore, Muhammad Fiaz *et al.* synthesized high efficient oxygen evolution reaction (OER) catalyst NiS@MOF-5, which can be coated on Ni-foam to form NiS@MOF-5/NF and showed OER catalytic activity and excellent stability.[10] Besides, Nguyenet *et al.* found that Ni-MOF-74 possessed ultrahigh catalytic activity for the arylation of azoles.[11]

Enzyme, also called biocatalyst, has the characteristics of high efficiency, specificity and mild reaction conditions.[12,13] Peroxidase is a kind of enzyme, which is widely existed in nature and can participate in the metabolism of organisms,[14] it can also be used for the diagnosis and detection of H_2O_2, glucose, ascorbic acid.[15,16] However, natural enzymes usually have drawbacks of the high cost of preparation and purification, special storage conditions and low stability.[15,17–20] The enzyme activity can only be best performed under suitable conditions, such as optimal temperature and acid-alkali conditions.[13,21,22] Therefore, people begin to pay attention to the research of artificial mimic peroxidase.[23–27]

It has been reported that Fe_3O_4 could catalyze the oxidation of TMB and OPDA to generate blue and orange color reactions, respectively.[28] Since then, many researchers have carried out research on the application of Fe_3O_4 mimic peroxidase in the field of glucose detection.[29,30] Later, it has been discovered that

[a]*Chemical Synthesis and Pollution Control Key Laboratory of Sichuan Province, College of Chemistry and Chemical Engineering, China West Normal University, Nanchong 637002, Sichuan, P. R. China. E-mail: zhwangs@163.com; Fax: +86 817-2445233; Tel: +86 817-2568081*

[b]*Yantai Institute of Materia Medica, Yantai 264000, Shandong, P. R. China. E-mail: cgren@yimm.ac.cn*

† Electronic supplementary information (ESI) available. See DOI: 10.1039/d1ra04877e

Co_3O_4 nanoparticles,[31] V_2O_5 nanowires,[32] CuO nanoparticles,[33] MnO_2 microspheres[34] and Ag_2O,[21] *etc.* also have intrinsic catalytic activity on classic peroxidase substrates in the presence of H_2O_2. At present, colorimetry is the most widely used method for glucose detection. The principle is that glucose oxidase (GOX) catalyzes the oxidation of glucose and the reduction of O_2 to H_2O_2, then the simulated peroxidase catalyzes H_2O_2 to produce hydroxyl free groups to oxidize substrates (TMB, DAB, OPDA, *etc.*) to produce color reaction.[35]

As a peroxidase mimetic enzyme, MOFs have substantive applications in colorimetric detection of some substances such as H_2O_2 and glucose. It has been reported that some iron-containing MOFs, such as MIL-53(Fe),[36] MIL-88(Fe)[37] and MIL-68(Fe)[38] possess the properties of peroxidase mimics. In the presence of H_2O_2, the hydrothermally synthesized MIL-53(Fe) can catalyze the oxidation of TMB and OPDA, which has been applied to the detection of actual samples such as glucose and serum with a good linear range and selectivity. Later, it was found that precious metals such as Au and other metals,[39] and composite metals (such as bimetallic) also have the catalytic activity of mimetic enzymes,[40] which makes MOFs as a popular new material in the simulation of peroxidase.

Several Cu-MOFs were reported previously that different organic compounds were used as coordination ligands, such as uric acid,[41] 2-aminoterephthalic acid[42] and 1,10-phenanthroline-2,9-dicarboxylic acid.[43] In this work, we prepared a Cu-MOF by using a simple hydrothermal method with 1,3,5-benzenetricarboxylic acid (H_3BTC) as ligand. The peroxidase-like activity of the as-prepared Cu-MOF was investigated by the oxidation reaction of TMB and OPDA with H_2O_2. The Cu-MOF showed high peroxidase-like activity, which can be used for catalyzing OPDA and TMB to generate colored products in the presence of H_2O_2. To investigate the possible oxidation mechanism of the Cu-MOF, typical Michaelis–Menten curves were obtained through steady-state kinetic experiments. Furthermore, the color reaction of TMB with H_2O_2 can be inhibited by some reductive substances. Based on these findings, we obtained satisfied results with the Cu-MOF for colorimetric detection of H_2O_2, ascorbic acid, sodium thiosulfate and glucose.

2. Experimental

2.1. Materials

1,3,5-Benzenetricarboxylic acid (H_3BTC) and TMB were obtained from Shanghai Titan Scientific Co, Ltd (Shanghai, China). OPDA, hydrogen peroxide (H_2O_2, 30%), copper nitrate trihydrate ($Cu(NO_3)_2 \cdot 3H_2O$), sodium acetate (NaAc), acetic acid (HAc), ethanol absolute, phosphate buffered saline (PBS), sodium hydroxide (NaOH), hydrochloric acid (HCl), GOX, glucose, maltose, lactose, sucrose were obtained from Chendu Kelong Chemical Reagent Company. All the reagents were of analytical reagent grade and all the aqueous solutions were prepared with deionized water.

2.2. Characterizations

X-ray powder diffraction (XRD) spectroscopy was performed on Rigaku Dmax/Ultima LV X-ray powder diffractometer. Fourier transform infrared (FT-IR) spectrometer (Nicolet-6700) was applied to record FTIR spectroscopy. Scanning electron microscopy (SEM) image and energy dispersive X-ray spectroscopy (EDS) image were taken by a Hitachi S4800 scanning electron microscope.

2.3. Cu-MOF preparation

The Cu-MOF was prepared by using hydrothermal method. Briefly, 0.45 g (2.14 mmol) H_3BTC was dissolved in 48 mL absolute ethanol and stirred for 10 min. Next, addition of 0.75 g (3.1 mmol) of $Cu(NO_3)_2 \cdot 3H_2O$ to the above solution and continued stirring for 10 min. Then, transferred the mixed solution into a Teflon-lined stainless autoclave. After heated at 120 °C for 12 h and cooled down to the room temperature, collected the Cu-MOF by centrifugation and washed 3 times with absolute ethanol, then dried in a vacuum drying-oven for 24 h at 60 °C to obtain the target product.[44]

2.4. Peroxidase-like activity

The catalytic oxidation of TMB by H_2O_2 was performed in 100 mM acetate buffer (pH 4.0) in the presence of Cu-MOF catalyst. Briefly, 2.4 mL of 0.06 mg mL^{-1} Cu-MOF (Cu-MOF solid was dispersed in acetate buffer by ultrasonication), 300 μL TMB (0.3 mM, dissolve the DMF) and 300 μL H_2O_2 (0.6 mM) were mixed and reacted for 20 min at 30 °C. The maximum absorption wavelength of TMB oxidized product (652 nm)[45] was measured with a UV-Vis spectrophotometer. For OPDA oxidation, 1 mL of 0.06 mg mL^{-1} Cu-MOF solution (Cu-MOF solid was dispersed in deionized water), 1 mL OPDA (0.4 mM, dissolve the deionized water) and 1 mL H_2O_2 (0.6 mM) were reacted for 20 min at 30 °C. The maximum absorption wavelength of OPDA oxidized product (416 nm)[15] was measured by a UV-Vis spectrophotometer.

2.5. Cu-MOF kinetics measurements

First, 6 mg Cu-MOF solid was dispersed in 100 mL acetate buffer (pH 4.0) to prepare 0.06 mg mL^{-1} Cu-MOF solution. The concentration of the TMB was fixed at 0.2 mM and a series of H_2O_2 with different concentrations (10 mM–90 mM) were prepared. During the reaction, 2.6 mL Cu-MOF solution, 0.1 mL H_2O_2 solution and 0.3 mL TMB were mixed with a total volume of 3 mL at 30 °C. The reaction product was sampled at regular intervals and spectroscopically detected at 652 nm by using a UV-Vis spectrophotometer. Similar experiments were performed by varying the concentration of TMB (0.1 mM–0.9 mM) with fixed concentration of H_2O_2 (3.5 mM).

For OPDA oxidation, 6 mg Cu-MOF solid was dispersed in 100 mL 0.1 M PBS buffer (pH 7.4) to prepare 0.06 mg mL^{-1} Cu-MOF solution. The concentration of OPDA was fixed at 0.4 mM with a series of concentration of H_2O_2 solutions (0.02 mM–0.6 mM). During the reaction, 1 mL Cu-MOF solution, 1 mL H_2O_2 and 1 mL OPDA were mixed with a total volume of 3 mL at 30 °C. The reaction product was sampled at regular intervals and spectroscopically detected at 416 nm by a UV-vis spectrophotometer. Similar measurements were carried out by varying the concentration of OPDA (0.05 mM–1 mM) with fixed

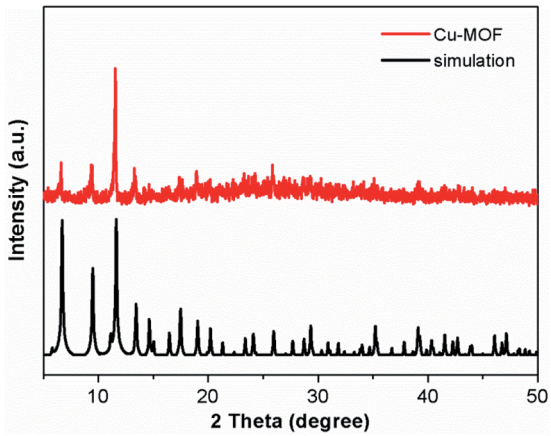

Fig. 1 The XRD pattern of Cu-MOF.

concentration of H_2O_2 (0.6 mM). By monitoring the absorbance at 652 nm and 416 nm for TMB and OPDA oxidation, the steady-state reaction rates were obtained with the Lambert Beer's law: $A = \varepsilon \times b \times C$. A is absorbance which can be measured; ε is the molar extinction coefficient of OPDA oxidation product ($\varepsilon = 16.7$ mM^{-1} cm^{-1})[46] and TMB oxidation product ($\varepsilon = 39$ mM^{-1} cm^{-1}),[47] b is the path length of light ($b = 1$ cm). The rate V can be calculated by the change of concentration with time: $V = \Delta c/\Delta t$. Michaelis–Menten equation, $V = V_{max}[S]/(K_m + [S])$, was used to obtain the apparent kinetic parameters by nonlinear least square fitting the absorbance data. The V_{max} is the reaction velocity of an enzyme with saturated substrate. K_m is so called Michaelis constant, which represents the substrate concentration when enzymatic reaction velocity V reaches the half of the V_{max}. Usually, the V_{max} and K_m values can be determined by Lineweaver–Burk double reciprocal model ($1/V = (K_m/V_{max})\cdot(1/[S]) + 1/V_{max}$). A straight line is formed by plotting $1/V$ as a function of $1/[S]$, and the intercept of this line on X axis represents $-1/K_m$, and Y axis represents $1/V_{max}$.

The experimental procedures of the effects of pH, catalyst concentration and reaction temperature on the peroxidase-like activity of Cu-MOF, and the detection of H_2O_2, ascorbic acid, sodium thiosulfate and glucose were similar to the above-mentioned experimental process (see ESI† for details). The data presented in this work were the averages of at least two measurements with an error less than 5% unless otherwise stated.

3. Results and discussions

3.1. Characterizations

The XRD pattern of the Cu-MOF is shown in Fig. 1. The characteristic peaks at $2\theta = 6.7°$, 9.5°, 11.6°, 13.4°, 14.9°, 17.5°, 19.1°, 25.9° and 39.1° correspond to the (200), (220), (222), (400), (420), (511), (440), (731) and (882) crystal planes.[48–50] The narrow and sharp peaks and the main peaks are coincided well with the simulated peaks, which prove that the synthesized material is the target product. The SEM image shows that the Cu-MOF sample is mainly composed of polyhedron, and some irregular particles can also be seen on the surface of the sample (Fig. 2). The FTIR spectrum of Cu-MOF is shown in Fig. S1,† the peaks at 1370 cm^{-1} can be attributed to the aromatic ring extension. 690–900 cm^{-1} were assigned to the out-of-plane bending vibration of aromatic hydrocarbons C–H.[51] The absorption bands at 600–800 cm^{-1} are due to lattice vibrations of Cu–O, Cu–O–Cu and O–Cu–O. The stretching vibration of benzene ring is at 1579 cm^{-1}, whereas the peak at 3404 cm^{-1} can be ascribed to water molecules and hydroxyl groups on the surface of the sample.[51–55] The energy dispersive spectrum (EDS) and element mapping indicate that Cu, O and C elements are coexisted and distributed evenly in the sample (Fig. S2†).

3.2. Peroxidase activity

The peroxidase-like activity of the Cu-MOF was evaluated by the catalytic reaction of OPDA and TMB with H_2O_2. Fig. 3A shows that the Cu-MOF can catalyze H_2O_2 to oxidize OPDA at 30 °C, which produce a color product since the solution become yellow after the reaction (Fig. 3A, inset). The oxidation product of OPDA shows an absorption band at wavelength of 416 nm in the visible region (Fig. 3A). Besides, the Cu-MOF can also catalyze the oxidation of TMB by H_2O_2, and the oxidation product of TMB exhibited a broad absorption band at 652 nm in the visible region and a peak at 371 nm in the UV region (Fig. 3B). The color of the TMB solution changed to blue after oxidation by H_2O_2 (Fig. 3B, inset). The absorption peaks at 416 nm and 652 nm for

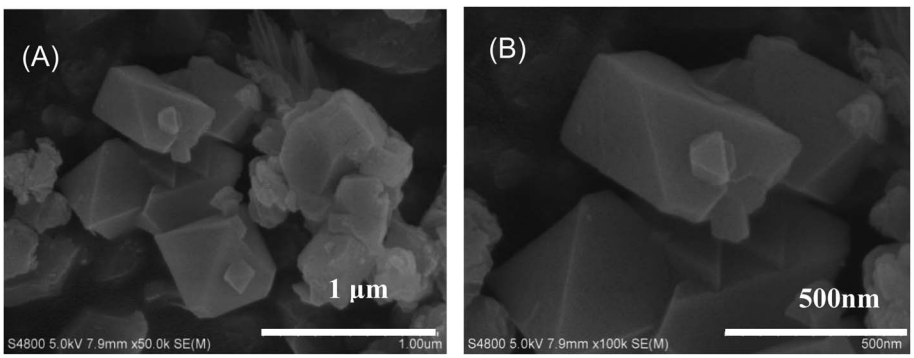

Fig. 2 The SEM images of Cu-MOF with different magnifications.

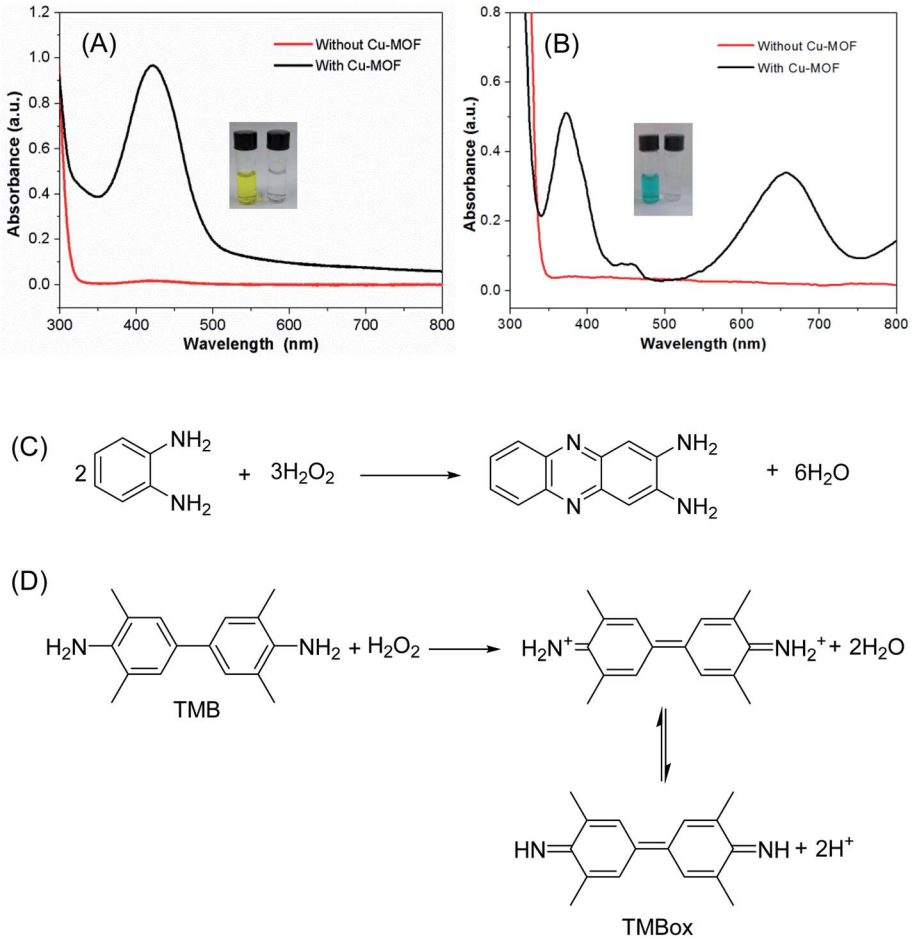

Fig. 3 The UV-Vis spectra of OPDA (A) and TMB (B) (insets: photographs of OPDA and TMB oxidized with H_2O_2) with and without Cu-MOF material. (C and D) Are the corresponding reaction equations for Cu-MOF catalyzed OPDA and TMB, respectively.

OPDA and TMB solutions, respectively, were not observed in the UV-Vis spectra without addition of Cu-MOF (Fig. 3A and B), and the corresponding solutions were still colorless (the little glass bottles on the right of the insets in Fig. 3A and B, respectively). These results proved that the colored products generated by the reaction of OPDA and TMB with H_2O_2 were indeed catalyzed by the Cu-MOF material.

Fig. 3C and D show the corresponding reaction equations for Cu-MOF catalyzed OPDA and TMB oxidation, respectively. In the presence of Cu-MOF as catalysts, OPDA and TMB are oxidized by H_2O_2, producing a yellow-colored dimer product (2,3-diaminophenazine) (Fig. 3C) and a blue oxidized product complex (Fig. 3D), and H_2O_2 is reduced to H_2O simultaneously. The 371 and 652 nm bands in the absorption spectrum of TMB oxidation product are a charge transfer complex consisting of the diamine (TMB) as a donor and the diimine dication (TMB^{2+}) as an acceptor.[56,57]

3.3. Experimental condition optimization

Natural enzymes are easily inactivated under extreme conditions such as strong acid, strong base and high temperature. Herein, the effect of pH, temperature, and catalyst concentration were investigated for the peroxidase activity. First, we explored the effect of pH. For the OPDA, the reaction activity increased from pH 3.0 to pH 4.5, while decreased with further pH increase up to 9.0 (Fig. 4A), which similar to that of the peroxidase activity of HRP effected by pH. While for the TMB, the reaction activity increased from pH 3.0 to pH 4.0, while decreased with further increasing of the pH (Fig. 4B). We further investigated the effect of temperature on the peroxidase-like activity of Cu-MOF. It can be seen that the catalytic activity of Cu-MOF increased from 25 °C to 70 °C when oxidation of OPDA with H_2O_2 (Fig. 4C) and the activity of the enzyme was not lose even up to 70 °C. While the highest activity was at 30 °C for TMB oxidation, and the color of the oxidation product faded marvelously at 45 °C (Fig. 4D), which indicated that the enzyme had been inactivated. Finally, we studied the catalyst concentration effect and the results are shown in the Fig. 4E and F. The activity of OPDA oxidation increased linearly with the increase of catalyst between 0.03 and 0.06 mg mL^{-1}, which reached maximum at 0.06 mg mL^{-1} and then tends to be flat. However, the concentration of catalyst had little effect on the activity for the oxidation of TMB with the activity higher than 70% between 0.03 and 0.09 mg mL^{-1}.

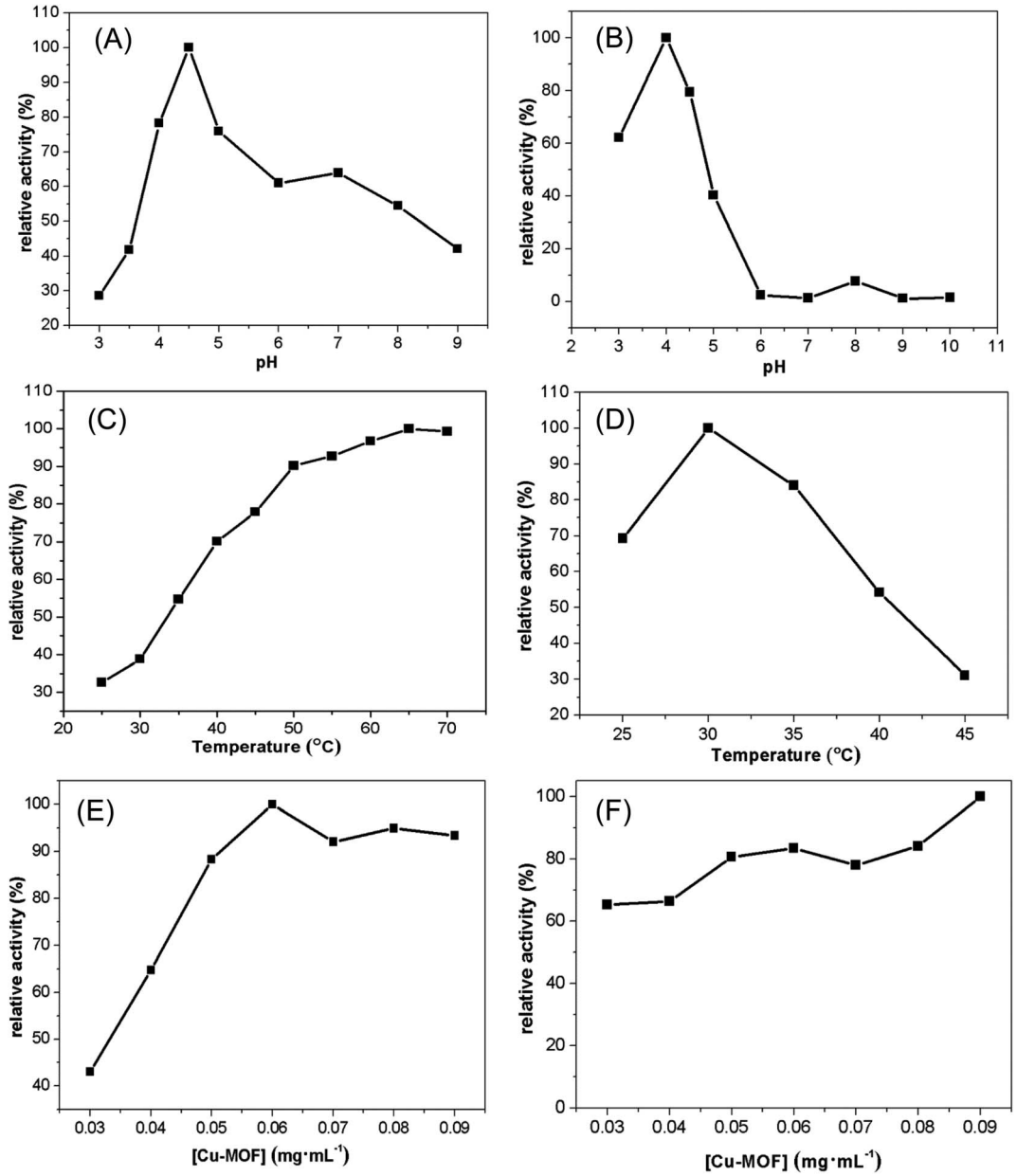

Fig. 4 The effect of pH for oxidation of OPDA (A) and TMB (B), temperature effect for oxidation of OPDA (C) and TMB (D), and the effect of catalyst concentration for oxidation of OPDA (E) and TMB (F).

3.4. Steady-state kinetics study

Steady-state kinetics assays were carried out to explore the mechanism of the peroxidase-like activity of the synthesized Cu-MOF. The kinetic data were measured by fixing concentration of H_2O_2 and varying the OPDA (or TMB) concentration or *vice versa* with Cu-MOF. The formation rates of the OPDA and TMB oxidized products were monitored from the increasing of the absorbance at 416 nm and 652 nm, respectively. The Fig. 5A showed the reaction rate of Cu-MOF peroxidase gradually increased with the increase of H_2O_2 when fixing OPDA. While when the H_2O_2 increases to a certain extent, the increasing rate of the reaction rate becomes slower and gradually flattens out. Secondly, when the concentration of H_2O_2 is fixed, the reaction rate of Cu-MOF peroxidase gradually increases with the increase of OPDA (Fig. 5B). However, when the concentration of OPDA increases to a certain extent, the reaction rate also gradually slows down. The fitting parameters (K_m and V_{max}) could be obtained through hyperbola curve fitting, which were shown in the Fig. 5C and D.

The steady-state kinetics of TMB oxidation by H_2O_2 catalyzed with Cu-MOF is shown in Fig. 6A. The reaction rate of TMB oxidation gradually increased with the increasing of H_2O_2 when fixing TMB. While when the H_2O_2 increases to a certain extent, the increasing of the reaction rate becomes slower and gradually flattens out. Secondly, when the concentration of H_2O_2 is fixed, the reaction rate of Cu-MOF peroxidase gradually

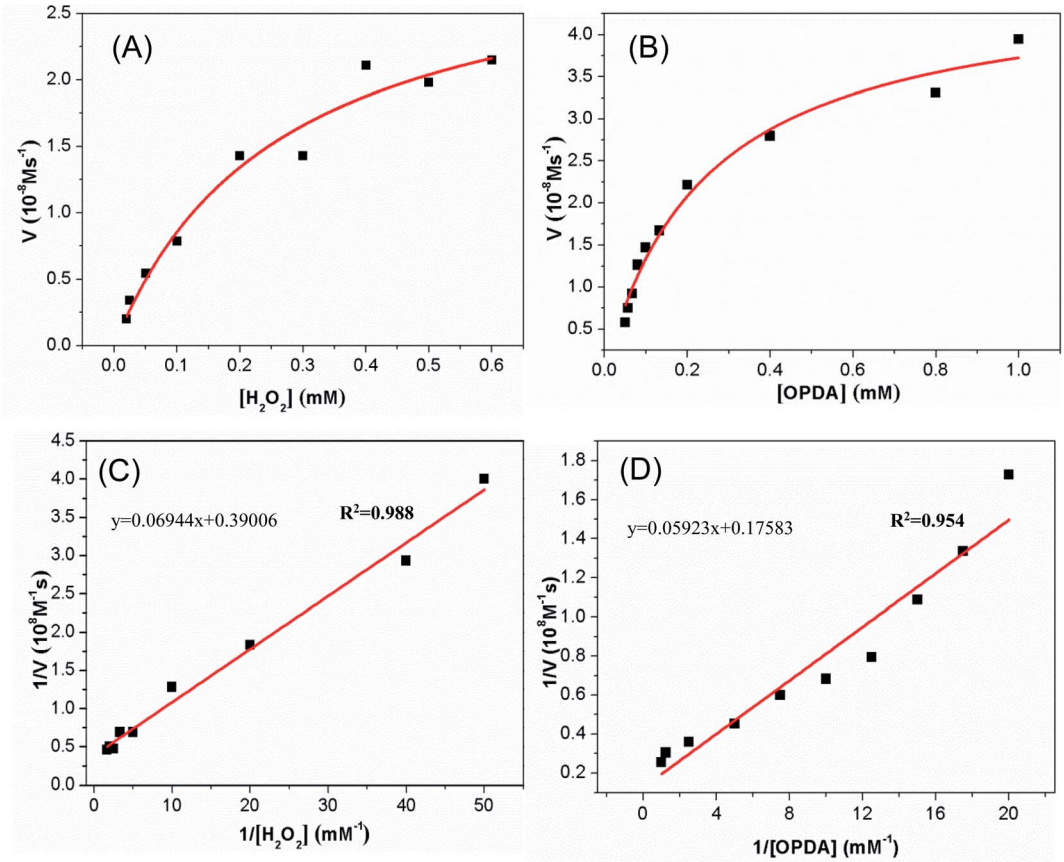

Fig. 5 Steady-state kinetics for the reaction of OPDA with H_2O_2 in the present of Cu-MOF. (A and C) Fixed OPDA concentration (0.4 mM) and varied H_2O_2 concentration (0.02 mM–0.6 mM); (B and D) fixed H_2O_2 concentration (0.6 mM) and varied OPDA concentration (0.05 mM–1 mM). The curves in panels A and B were obtained by nonlinear least square fitting to Michaelis–Menten equation, $V = V_{max}\cdot[S]/(K_m + [S])$, and the lines in panels C and D were obtained by linear least square fitting to Lineweaver–Burk double reciprocal model, $1/V = (K_m/V_{max})\cdot(1/[S]) + 1/V_{max}$.

increases with the increase of TMB (Fig. 6B). However, when the concentration of TMB increases to a certain extent, the reaction rate also gradually slows down. By using the Lineweave–Burk double-reciprocal model to fit the data in the Michaelis curve, the straight lines can be obtained as shown in the Fig. 6C and D.

The kinetic parameters K_m and V_{max} for the catalyst of Cu-MOF were calculated through the intercept and slope in the straight line. Tables S1 and S2† list the K_m and V_{max} values of several catalysts for substrates OPDA, TMB and H_2O_2. K_m value is one of the characteristic constant of enzymes, which indicates the affinity between enzyme and substrate. The higher the K_m value, the smaller the affinity between enzyme and substrate. These results showed that the K_m values of the Cu-MOF for OPDA and TMB were 0.54 mM and 0.456 mM, respectively. And the K_m values of natural HRP for OPDA and TMB were 0.59 mM and 0.434 mM, respectively.[28,58] Therefore, the affinity of Cu-MOF was similar to that of natural HRP, indicating it can be used as an artificial peroxidase. Through further comparison, we found that the affinity of Cu-MOF for OPDA and TMB is better than some of the published peroxidase mimetic materials, such as the affinity of Fe_3O_4@Cu@Cu_2O to OPDA and the affinity of Cu NCs or MoO_2 to TMB (Tables S1 and S2†).

3.5. Colorimetric detection of H_2O_2, ascorbic acid and sodium thiosulfate

The oxidation of TMB by H_2O_2 *via* the catalysis of Cu-MOF to generate a blue product, and the reaction rate was proportional to the concentration of H_2O_2. Based on this principle, a colorimetric method to detect H_2O_2 was established. As shown in Fig. 7A, the absorbance at 652 nm increased with the concentration increasing of H_2O_2 from 5 μM to 400 μM. A well linear relationship can be achieved between the absorbance intensity and H_2O_2 concentration from 5 μM to 300 μM (Fig. 7B). The detection limit was 4.6 μM and the correlation coefficient was 0.997. The detection limit was determined by LOD = KS_0/S. K is the numerical factor chosen on the basis of the confidence level desired. S_0 is the standard deviation[59] of the blank measurements ($n = 11$, $K = 3$), while S is the slope of the calibration curve. Table S3† list several peroxidase mimics for colorimetric detection of H_2O_2. According to the Table S3,† the linear range of the as-prepared Cu-MOF is wider than some of the published peroxidase mimics such as CuS-GNS,[60] and the detect limitation is also lower than some reported peroxidase mimics such as MnO_2,[58] indicated that Cu-MOF is suitable for the colorimetric detection of H_2O_2.

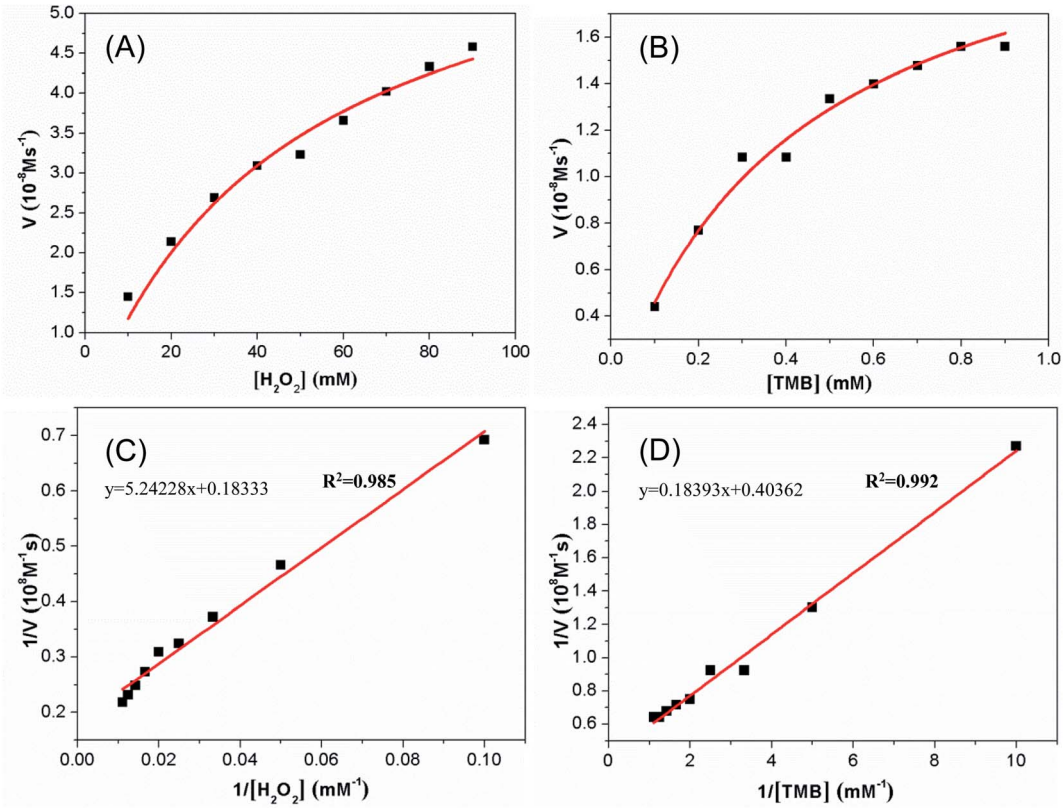

Fig. 6 Steady-state kinetics for the reaction of TMB with H_2O_2 in the present of Cu-MOF. (A and C) Fixed TMB concentration (0.2 mM) and varied H_2O_2 concentration (10 mM–90 mM); (B and D) fixed H_2O_2 concentration (3.5 mM) and varied TMB concentration (0.1 mM–0.9 mM). The curves in panels A and B and the lines in panels C and D were obtained as stated in Fig. 5.

Moreover, it was found that the color reaction of TMB with H_2O_2 could be inhibited by ascorbic acid (AA) and sodium thiosulfate ($Na_2S_2O_3$). Accordingly, a colorimetric detection method of AA and $Na_2S_2O_3$ was also developed based on the color reaction inhibition (ESI, Fig. S3 and S4†). It should be pointed out that the detection of AA and $Na_2S_2O_3$ is not specific, for other reductive substance such as Na_2SO_3 can also inhibit the color reaction of TMB with H_2O_2.[21,61]

3.6. Glucose detection

GOX is a typical oxidoreductase that can be used to catalyze the oxidation of glucose to produce glucono-δ-lactone and H_2O_2.[62] It can be used in clinical diagnosis, rapid and accurate determination of glucose content in body fluid, which provides reliable data for doctors to accurately judge the patient's condition.[37,63,64] As shown in the Fig. 8A and B, the absorbance at 652 nm for TMB oxidation increased with the glucose

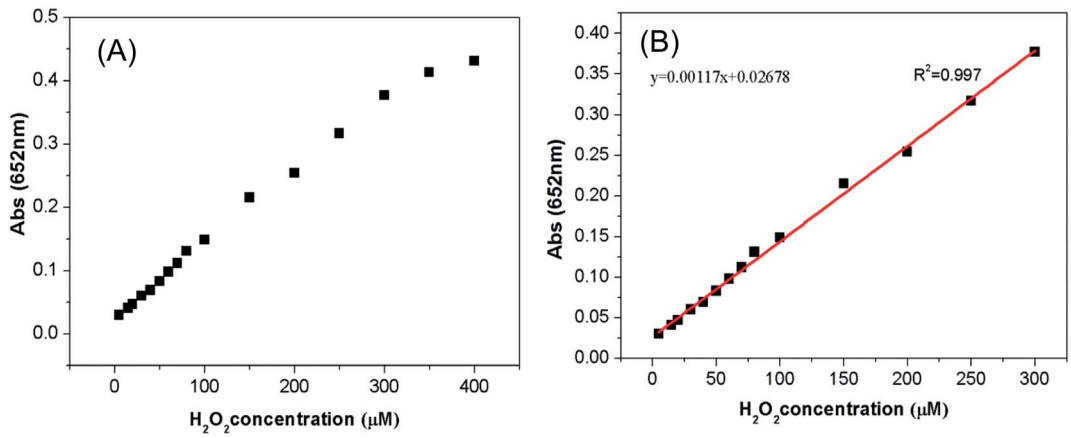

Fig. 7 Colorimetric detection of H_2O_2. Dose–response curve (A) and linear calibration plot (B) for the detection of H_2O_2 with Cu-MOF.

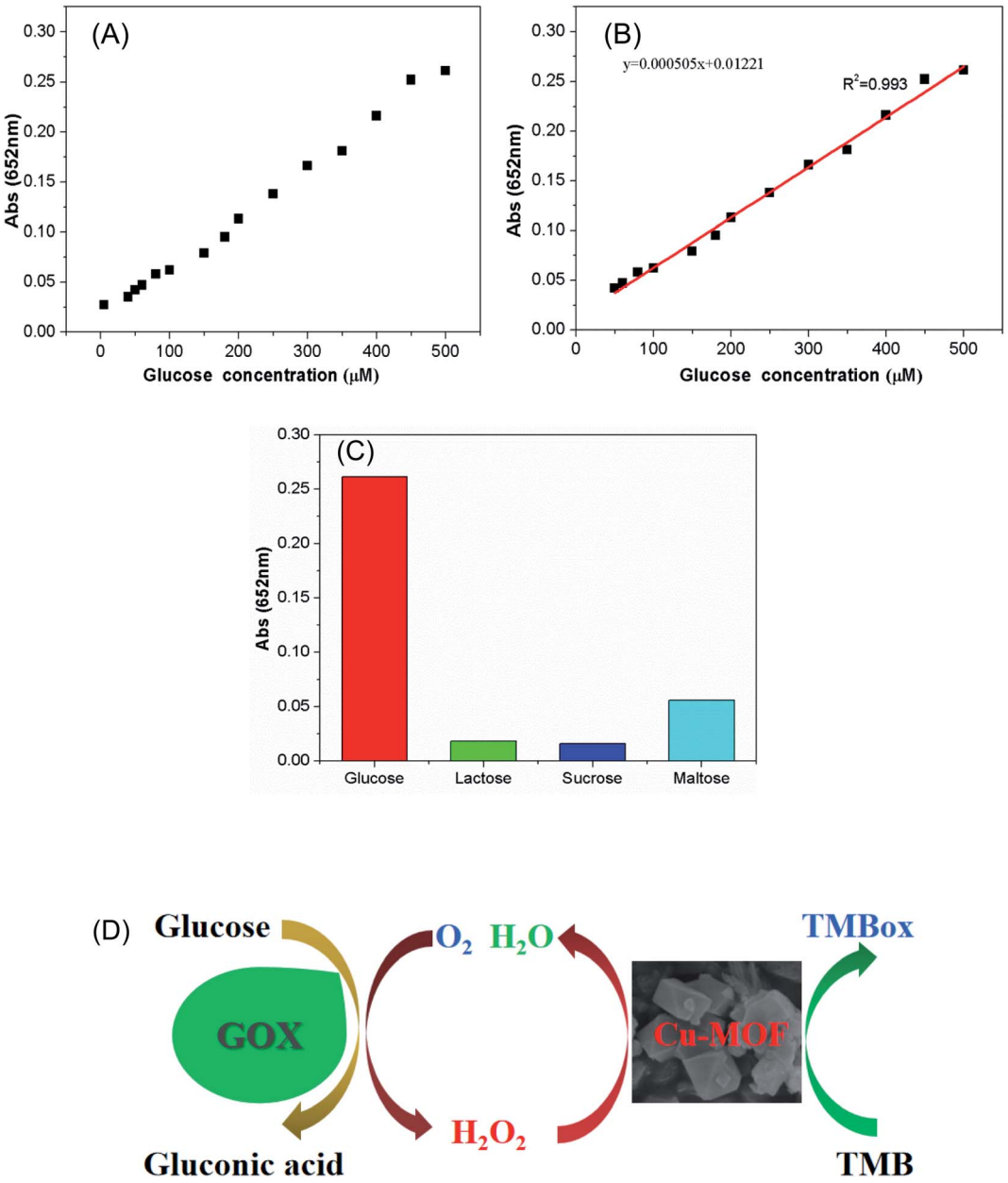

Fig. 8 The colorimetric detection of glucose. Dose–response curve (A) and linear calibration plot (B) for glucose detection with Cu-MOF. (C) Determination of the selectivity detection for glucose with 300 μM glucose, 2 mM sucrose, 2 mM lactose, and 2 mM maltose. (D) A proposed reaction mechanism for detection of glucose.

concentration from 5 μM to 500 μM. A well linear relationship can be obtained between the intensity of absorbance and the glucose concentration from 5 μM to 500 μM. The detection limit is 4.7 μM and the correlation coefficient is 0.993.

To explore the selectivity of glucose detection, we performed the colorimetric reaction by replacing glucose with other sugar species, such as sucrose, lactose or maltose. The results show that the absorbance increase at 652 nm is very low for the selected sugar species instead of glucose (Fig. 8C). Therefore, the developed colorimetric detection method has high selectivity for the detection of glucose.

The reaction mechanism for glucose detection is illustrated in Fig. 8D. First, GOX catalyzed the oxidation of glucose to gluconic acid and O_2 dissolved in the solution was reduced to H_2O_2. Then the produced H_2O_2 oxidized TMB to a blue-colored oxidation product (TMBox) *via* the catalysis of Cu-MOF. The production of TMBox is proportional to the amount of H_2O_2, and the yield of H_2O_2 is proportional to the amount of glucose. Therefore, the production of TMBox is proportional to the amount of glucose and glucose can be detected by measuring the amount of TMBox. It also can be seen from the reaction mechanism that the detection of glucose is achieved by measuring the content of H_2O_2, thus the selectivity of glucose

detection depends on the selectivity of GOX to glucose, but not on the catalysis of Cu-MOF.

Table S4† listed several peroxidase mimic catalysts for the colorimetric detection of glucose. According to the Table S4,† the linear range of the as-prepared Cu-MOF is wider than that of $NiFe_2O_4$ MNPs and Ch-Ag NPs.[65,66] The detection limit is relatively large, which indicated that Cu-MOF has better linear range and detection limit to detect glucose. These results demonstrated that this colorimetric method may has potential application for determine glucose concentration.

4. Conclusion

In conclusion, we prepared Cu-MOF with high peroxidase-like activity by a simple hydrothermal method. In the presence of H_2O_2, Cu-MOF can catalyze the oxidation of OPDA and TMB. Kinetics studies suggested that the affinity of Cu-MOF to TMB and OPDA is close to that of HRP. Based on the color reaction of TMB with H_2O_2, colorimetric methods for the detection of H_2O_2 and glucose were established. Moreover, the detection of ascorbic acid and sodium thiosulfate was also performed upon the inhibition of TMB oxidation. These results indicate that Cu-MOF based peroxidase-like activity may be applied in the fields of catalysis, biosensor, food detection and environmental monitoring.

Conflicts of interest

There are no conflicts to declare.

Acknowledgements

This study was funded by the Open Project of Chemical Synthesis and Pollution Control Key Laboratory of Sichuan Province (CSPC2016-3-2), and the Opening Project of Key Laboratory of Green Chemistry of Sichuan Institutes of Higher Education (LZJ2002).

References

1 D. Li, S. Zhang, X. Feng, H. Yang, F. Nie and W. Zhang, A novel peroxidase mimetic Co-MOF enhanced luminol chemiluminescence and its application in glucose sensing, *Sens. Actuators, B*, 2019, **296**, 126631.

2 K. Shen, X. Chen, J. Chen and Y. Li, Development of MOF-derived carbon-based nanomaterials for efficient catalysis, *ACS Catal.*, 2016, **6**, 5887–5903.

3 L. E. Kreno, K. Leong, O. K. Farha, M. Allendorf, R. P. Van Duyne and J. T. Hupp, Metal–organic framework materials as chemical sensors, *Chem. Rev.*, 2012, **112**, 1105–1125.

4 D. Saha, H. A. Grappe, A. Chakraborty and G. Orkoulas, Postextraction separation, on-board storage, and catalytic conversion of methane in natural gas: a review, *Chem. Rev.*, 2016, **116**, 11436–11499.

5 D. Cunha, M. Ben Yahia, S. Hall, S. R. Miller, H. Chevreau, E. Elkaïm, G. Maurin, P. Horcajada and C. Serre, Rationale of drug encapsulation and release from biocompatible porous metal–organic frameworks, *Chem. Mater.*, 2013, **25**, 2767–2776.

6 G. Maurin, C. Serre, A. Cooper and G. Férey, The new age of MOFs and of their porous-related solids, *Chem. Soc. Rev.*, 2017, **46**, 3104–3107.

7 L. Chen, R. Luque and Y. Li, Controllable design of tunable nanostructures inside metal–organic frameworks, *Chem. Soc. Rev.*, 2017, **46**, 4614–4630.

8 D. Feng, T.-F. Liu, J. Su, M. Bosch, Z. Wei, W. Wan, D. Yuan, Y.-P. Chen, X. Wang and K. Wang, Stable metal-organic frameworks containing single-molecule traps for enzyme encapsulation, *Nat. Commun.*, 2015, **6**, 1–8.

9 Y. Qin, X. Han, Y. Li, A. Han, W. Liu, H. Xu and J. Liu, Hollow Mesoporous Metal–Organic Frameworks with Enhanced Diffusion for Highly Efficient Catalysis, *ACS Catal.*, 2020, **10**, 5973–5978.

10 M. Fiaz, M. Kashif, M. Fatima, S. R. Batool, M. A. Asghar, M. Shakeel and M. Athar, Synthesis of Efficient TMS@MOF-5 Catalysts for Oxygen Evolution Reaction, *Catal. Lett.*, 2020, **150**, 2648–2659.

11 H. T. Nguyen, D. N. Doan and T. Truong, Unprecedented salt-promoted direct arylation of acidic sp^2 CH bonds under heterogeneous Ni-MOF-74 catalysis: synthesis of bioactive azole derivatives, *J. Mol. Catal. A: Chem.*, 2017, **426**, 141–149.

12 S. K. Maji, A. K. Dutta, S. Dutta, D. N. Srivastava, P. Paul, A. Mondal and B. Adhikary, Single-source precursor approach for the preparation of CdS nanoparticles and their photocatalytic and intrinsic peroxidase like activity, *Appl. Catal., B*, 2012, **126**, 265–274.

13 P. V. Iyer and L. Ananthanarayan, Enzyme stability and stabilization—aqueous and non-aqueous environment, *Process Biochem.*, 2008, **43**, 1019–1032.

14 M. Yuan, H. Zhao, Q. Huang, X. Liu, Y. Zhou, X. Diao and Q. X. Li, Comparison of three palm tree peroxidases expressed by Escherichia coli: Uniqueness of African oil palm peroxidase, *Protein Expression Purif.*, 2020, **179**, 105806.

15 Z. Wang, M. Chen, J. Shu and Y. Li, One-step solvothermal synthesis of Fe_3O_4@Cu@Cu_2O nanocomposite as magnetically recyclable mimetic peroxidase, *J. Alloys Compd.*, 2016, **682**, 432–440.

16 Q. Wang, S. Liu, H. Sun and Q. Lu, Synthesis and Intrinsic Peroxidase-Like Activity of Sisal-Like Cobalt Oxide Architectures, *Ind. Eng. Chem. Res.*, 2014, **53**, 7917–7922.

17 Y. Chen, H. Cao, W. Shi, H. Liu and Y. Huang, Fe–Co bimetallic alloy nanoparticles as a highly active peroxidase mimetic and its application in biosensing, *Chem. Commun.*, 2013, **49**, 5013–5015.

18 M. Chen, Z. H. Wang, J. X. Shu, X. H. Jiang, W. Wang, Z. H. Shi and Y. W. Lin, Mimicking a Natural Enzyme System: Cytochrome c Oxidase-Like Activity of Cu_2O Nanoparticles by Receiving Electrons from Cytochrome c, *Inorg. Chem.*, 2017, **56**, 9400–9403.

19 Y. W. Lin, Rational design of heme enzymes for biodegradation of pollutants toward a green future, *Biotechnol. Appl. Biochem.*, 2020, **67**, 484–494.

20 Y.-l. Dong, H.-g. Zhang, Z. U. Rahman, L. Su, X.-j. Chen, J. Hu and X.-g. Chen, Graphene oxide–Fe 3 O 4 magnetic nanocomposites with peroxidase-like activity for colorimetric detection of glucose, *Nanoscale*, 2012, **4**, 3969–3976.

21 W. Lu, J. Shu, Z. Wang, N. Huang and W. Song, The intrinsic oxidase-like activity of Ag_2O nanoparticles and its application for colorimetric detection of sulfite, *Mater. Lett.*, 2015, **154**, 33–36.

22 M. Chen, Z. Wang, J. Shu, X. Jiang, W. Wang, Z.-H. Shi and Y.-W. Lin, Mimicking a natural enzyme system: cytochrome c oxidase-like activity of Cu_2O nanoparticles by receiving electrons from cytochrome c, *Inorg. Chem.*, 2017, **56**, 9400–9403.

23 S. Maeno, Y. Mizutani, Q. Zhu, T. Miyamoto, M. Fukushima and H. Kuramitz, The oxidation of tetrabromobisphenol A by potassium monopersulfate with an iron(III)-phthalocyanine-tetrasulfonic acid catalyst in the presence of humic acid, *J. Environ. Sci. Health, Part A: Toxic/Hazard. Subst. Environ. Eng.*, 2014, **49**, 981–987.

24 T. Ying, F. Zhong, Z. H. Wang, J. Xie, X. Tan and Z. X. Huang, Generation of novel functional metalloproteins *via* hybrids of cytochrome c and peroxidase, *Protein Eng., Des. Sel.*, 2013, **26**, 401–407.

25 I. Artaud, K. Ben-Aziza and D. Mansuy, Iron porphyrin-catalyzed oxidation of 1, 2-dimethoxyarenes: a discussion of the different reactions involved and the competition between the formation of methoxyquinones or muconic dimethyl esters, *J. Org. Chem.*, 1993, **58**, 3373–3380.

26 C. Liu, J. K. Xu, S. Q. Gao, B. He, C. W. Wei, X. J. Wang, Z. H. Wang and Y. W. Lin, Green and efficient biosynthesis of indigo from indole by engineered myoglobins, *RSC Adv.*, 2018, **8**, 33325–33330.

27 J. J. X. Wu, X. Y. Wang, Q. Wang, Z. P. Lou, S. R. Li, Y. Y. Zhu, L. Qin and H. Wei, Nanomaterials with enzyme-like characteristics (nanozymes): next-generation artificial enzymes (II), *Chem. Soc. Rev.*, 2019, **48**, 1004–1076.

28 L. Gao, J. Zhuang, L. Nie, J. Zhang, Y. Zhang, N. Gu, T. Wang, J. Feng, D. Yang, S. Perrett and X. Yan, Intrinsic peroxidase-like activity of ferromagnetic nanoparticles, *Nat. Nanotechnol.*, 2007, **2**, 577–583.

29 S. Song, Y. Liu, A. Song, Z. Zhao, H. Lu and J. Hao, Peroxidase mimetic activity of Fe_3O_4 nanoparticle prepared based on magnetic hydrogels for hydrogen peroxide and glucose detection, *J. Colloid Interface Sci.*, 2017, **506**, 46–57.

30 Y. Shi, J. Huang, J. Wang, P. Su and Y. Yang, A magnetic nanoscale Fe_3O_4/Pβ-CD composite as an efficient peroxidase mimetic for glucose detection, *Talanta*, 2015, **143**, 457–463.

31 J. Mu, Y. Wang, M. Zhao and L. Zhang, Intrinsic peroxidase-like activity and catalase-like activity of Co3O4 nanoparticles, *Chem. Commun.*, 2012, **48**, 2540–2542.

32 R. André, F. Natálio, M. Humanes, J. Leppin, K. Heinze, R. Wever, H. C. Schröder, W. E. G. Müller and W. Tremel, V_2O_5 Nanowires with an Intrinsic Peroxidase-Like Activity, *Adv. Funct. Mater.*, 2011, **21**, 501–509.

33 W. Chen, J. Chen, Y. B. Feng, L. Hong, Q. Y. Chen, L. F. Wu, X. H. Lin and X. H. Xia, Peroxidase-like activity of water-soluble cupric oxide nanoparticles and its analytical application for detection of hydrogen peroxide and glucose, *Analyst*, 2012, **137**, 1706–1712.

34 M. Chen, J. Shu, Z. Wang and C. Ren, Porous surface MnO_2 microspheres as oxidase mimetics for colorimetric detection of sulfite, *J. Porous Mater.*, 2016, **24**, 973–977.

35 F. Qiao, L. Chen, X. Li, L. Li and S. Ai, Peroxidase-like activity of manganese selenide nanoparticles and its analytical application for visual detection of hydrogen peroxide and glucose, *Sens. Actuators, B*, 2014, **193**, 255–262.

36 L. Ai, L. Li, C. Zhang, J. Fu and J. Jiang, MIL-53(Fe): a metal-organic framework with intrinsic peroxidase-like catalytic activity for colorimetric biosensing, *Chem.–Eur. J*, 2013, **19**, 15105–15108.

37 Y. L. Liu, X. J. Zhao, X. X. Yang and Y. F. Li, A nanosized metal-organic framework of Fe-MIL-88NH($_2$) as a novel peroxidase mimic used for colorimetric detection of glucose, *Analyst*, 2013, **138**, 4526–4531.

38 F. Jing, R. Liang, J. Xiong, R. Chen, S. Zhang, Y. Li and L. Wu, MIL-68(Fe) as an efficient visible-light-driven photocatalyst for the treatment of a simulated waste-water contain Cr(VI) and Malachite Green, *Appl. Catal., B*, 2017, **206**, 9–15.

39 Y. Jv, B. Li and R. Cao, Positively-charged gold nanoparticles as peroxidase mimic and their application in hydrogen peroxide and glucose detection, *Chem. Commun.*, 2010, **46**, 8017–8019.

40 H. Yang, R. Yang, P. Zhang, Y. Qin, T. Chen and F. Ye, A bimetallic (Co/2Fe) metal-organic framework with oxidase and peroxidase mimicking activity for colorimetric detection of hydrogen peroxide, *Microchim. Acta*, 2017, **184**, 4629–4635.

41 F. Liu, J. He, M. Zeng, J. Hao, Q. Guo, Y. Song and L. Wang, Cu–hemin metal-organic frameworks with peroxidase-like activity as peroxidase mimics for colorimetric sensing of glucose, *J. Nanopart. Res.*, 2016, **18**, 106.

42 S. Wang, W. Deng, L. Yang, Y. Tan, Q. Xie and S. Yao, Copper-based metal–organic framework nanoparticles with peroxidase-like activity for sensitive colorimetric detection of Staphylococcus aureus, *ACS Appl. Mater. Interfaces*, 2017, **9**, 24440–24445.

43 J. Wang, Y. Hu, Q. Zhou, L. Hu, W. Fu and Y. Wang, Peroxidase-like Activity of Metal-Organic Framework [Cu(PDA)(DMF)] and Its Application for Colorimetric Detection of Dopamine, *ACS Appl. Mater. Interfaces*, 2019, **11**, 44466–44473.

44 W. Xuan, R. Ramachandran, C. Zhao and F. Wang, Influence of synthesis temperature on cobalt metal-organic framework (Co-MOF) formation and its electrochemical performance towards supercapacitor electrodes, *J. Solid State Electrochem.*, 2018, **22**, 3873–3881.

45 W. Dong, Y. Zhuang, S. Li, X. Zhang, H. Chai and Y. Huang, High peroxidase-like activity of metallic cobalt nanoparticles encapsulated in metal–organic frameworks derived carbon for biosensing, *Sens. Actuators, B*, 2018, **255**, 2050–2057.

46 S. Fornera and P. Walde, Spectrophotometric quantification of horseradish peroxidase with o-phenylenediamine, *Anal. Biochem.*, 2010, **407**, 293–295.
47 P. D. Josephy, T. Eling and R. P. Mason, The horseradish peroxidase-catalyzed oxidation of 3, 5, 3', 5'-tetramethylbenzidine. Free radical and charge-transfer complex intermediates, *J. Biol. Chem.*, 1982, **257**, 3669–3675.
48 R. Kaur, A. Kaur, A. Umar, W. A. Anderson and S. K. Kansal, Metal organic framework (MOF) porous octahedral nanocrystals of Cu-BTC: Synthesis, properties and enhanced adsorption properties, *Mater. Res. Bull.*, 2019, **109**, 124–133.
49 J. Zhou, D. Liu, Y. Xiong and Y. Akinay, A novel approach to prepare polyaniline/Polypyrrole@Cu-BTC/NH2-MIL-101(Fe) MOFs for electromagnetic wave absorption, *Ceram. Int.*, 2020, **46**, 19758–19766.
50 Y.-F. Zhang, L.-G. Qiu, Y.-P. Yuan, Y.-J. Zhu, X. Jiang and J.-D. Xiao, Magnetic Fe_3O_4@C/Cu and Fe_3O_4@CuO core–shell composites constructed from MOF-based materials and their photocatalytic properties under visible light, *Appl. Catal., B*, 2014, **144**, 863–869.
51 Q. Zhao, L. Zhu, G. Lin, G. Chen, B. Liu, L. Zhang, T. Duan and J. Lei, Controllable Synthesis of Porous Cu-BTC@polymer Composite Beads for Iodine Capture, *ACS Appl. Mater. Interfaces*, 2019, **11**, 42635–42645.
52 R. M. Abdelhameed, H. E. Emam, J. Rocha and A. M. S. Silva, Cu-BTC metal-organic framework natural fabric composites for fuel purification, *Fuel Process. Technol.*, 2017, **159**, 306–312.
53 V. Jabbari, J. M. Veleta, M. Zarei-Chaleshtori, J. Gardea-Torresdey and D. Villagrán, Green synthesis of magnetic MOF@GO and MOF@CNT hybrid nanocomposites with high adsorption capacity towards organic pollutants, *Chem. Eng. J.*, 2016, **304**, 774–783.
54 R. M. Abdelhameed, H. Abdel-Gawad, M. Elshahat and H. E. Emam, Cu–BTC@cotton composite: design and removal of ethion insecticide from water, *RSC Adv.*, 2016, **6**, 42324–42333.
55 T. J. Bandosz and C. Petit, MOF/graphite oxide hybrid materials: exploring the new concept of adsorbents and catalysts, *Adsorption*, 2010, **17**, 5–16.
56 Y. Misono, Y. Ohkata, T. Morikawa and K. Itoh, Resonance Raman and absorption spectroscopic studies on the electrochemical oxidation processes of 3, 3′, 5, 5′-tetramethylbenzidine, *J. Electroanal. Chem.*, 1997, **436**, 203–212.
57 X. Zhang, Q. Yang, Y. Lang, X. Jiang and P. Wu, Rationale of 3, 3′, 5, 5′-tetramethylbenzidine as the chromogenic substrate in colorimetric analysis, *Anal. Chem.*, 2020, **92**, 12400–12406.
58 X. Liu, Q. Wang, H. Zhao, L. Zhang, Y. Su and Y. Lv, BSA-templated MnO_2 nanoparticles as both peroxidase and oxidase mimics, *Analyst*, 2012, **137**, 4552–4558.
59 Y. Li, R. Cui, H. Huang, J. Dong, B. Liu, D. Zhao, J. Wang, D. Wang, H. Yuan, X. Guo and B. Sun, High performance determination of $Pb^{(2+)}$ in water by 2,4-dithiobiuret-Reduced graphene oxide composite with wide linear range and low detection limit, *Anal. Chim. Acta*, 2020, **1125**, 76–85.
60 G. Nie, L. Zhang, X. Lu, X. Bian, W. Sun and C. Wang, A one-pot and *in situ* synthesis of CuS-graphene nanosheet composites with enhanced peroxidase-like catalytic activity, *Dalton Trans.*, 2013, **42**, 14006–14013.
61 M. Chen, J. Shu, Z. Wang and C. Ren, Porous surface MnO_2 microspheres as oxidase mimetics for colorimetric detection of sulfite, *J. Porous Mater.*, 2017, **24**, 973–977.
62 F. Tan, Z. Wang, Y. Yang, X. Xie, X. Hua, X. Yang and H. Huang, Facile preparation of peroxidase-like core-shell nanorods and application as platform for colorimetric determination of glucose, insulin and glucose/insulin ratio, *Talanta*, 2019, **204**, 285–293.
63 Y. Long, Y. Pan, W. Zheng, D. Yi and H. Zheng, Supramolecular hydrogel-immobilized enzyme ficin as peroxidase mimics for colorimetric detection of glucose, *Microchem. J.*, 2020, **158**, 105276.
64 H. Q. Zheng, C. Y. Liu, X. Y. Zeng, J. Chen, J. Lu, R. G. Lin, R. Cao, Z. J. Lin and J. W. Su, MOF-808: A Metal-Organic Framework with Intrinsic Peroxidase-Like Catalytic Activity at Neutral pH for Colorimetric Biosensing, *Inorg. Chem.*, 2018, **57**, 9096–9104.
65 L. Su, W. Qin, H. Zhang, Z. U. Rahman, C. Ren, S. Ma and X. Chen, The peroxidase/catalase-like activities of $MFe_{(2)}O_{(4)}$ (M=Mg, Ni, Cu) MNPs and their application in colorimetric biosensing of glucose, *Biosens. Bioelectron.*, 2015, **63**, 384–391.
66 H. Jiang, Z. Chen, H. Cao and Y. Huang, Peroxidase-like activity of chitosan stabilized silver nanoparticles for visual and colorimetric detection of glucose, *Analyst*, 2012, **137**, 5560–5564.